WS05-D02

Joint Full Waveform Inversion of Diving Waves and Reflected Waves for Velocity Model Building

W. Zhou (ISTerre, Universite Grenoble Alpes), R. Brossier (ISTerre, Universite Grenoble Alpes), S. Operto (Geoazur, CNRS, Universite Nice-Sophia Antipolis) & J.M. Virieux* (Universite Joseph Fourier)

SUMMARY

At depths where there is no sampling by diving waves, FWI behaves as a least-squares migration of the short-spread reflections, hence providing a reconstruction of the short-scale reflectivity at the expense of the long wavelengths of the velocity. Recently, it has been proposed to modify the FWI formalism such that the long wavelengths of the velocity can be updated from reflected waves using some prior knowledge on the reflectivity and an explicit scale separation between the velocity macro-model and the reflectivity. This scale separation allows one to emphasize the forward-scattering regime in the sensitivity kernel of the FWI, referred to as reflection FWI (RFWI). The drawback of the RFWI is to discard the valuable information on the shallow subsurface carried out by diving waves. A new FWI formalism, referred to as joint FWI (JFWI) is proposed and takes advantage of the long-wavelength information carried out by both diving waves and reflected waves to build a smooth velocity model. This formalism leads to a workflow which iteratively cycles the
update of the smooth velocity model by JFWI and the update of the short-scale impedance model by classical FWI of short-spread reflections. Application to a synthetic Valhall model illustrates the performance of JFWI.

Introduction

With the emergence of long-offset wide-azimuth acquisitions and broadband sources, full waveform inversion (FWI) has been recognized as an efficient tool for velocity model building (Virieux and Operto (2009) for a review). For these long-offset experiments, FWI is mainly driven by the information carried out by diving waves and post-critical reflections to build the long-to-intermediate wavelengths of the velocity structure. Unfortunately, the penetration depths of diving waves are often insufficient to reach the deepest targeted structures, even for modern wide-azimuth surveys. At these depths, FWI behaves as a least-squares migration of the short-spread reflections rather than as a tool for velocity model building, introducing short-scale features in the velocity model. Depending on the level of accuracy of the initial model, these short-scale features are either artifacts resulting from the convergence toward a local minimum of the misfit function or migrated-like reconstruction of deep reflectors.
Alternatively, migration-based velocity analysis have been developed in the image domain to build velocity macromodel from reflection data. These approaches focus on the flattening of the common image gathers generated by migration (Symes and Carazzone, 1991; Sava and Biondi, 2004). Extended-domain approaches have also been proposed, which attempt to minimize the energy left in non-physical dimensions added to the model space (Sava and Fomel, 2006; Yang and Sava, 2011; Almomin and Biondi, 2012; Biondi and Almomin, 2012; Sun and Symes, 2012). The main issue of these approaches is their high computational cost and only 2D applications have shown promising results.

Scale separation in FWI

Inspired by the pioneering work of Chavent et al. (1994), recent data-domain FWI strategies, referred to as reflection FWI (RFWI) (e.g., Xu et al., 2012; Ma and Hale, 2013; Brossier et al., 2014), provide a new alternative to build velocity macromodel from reflection data. As most of the seismic reflection processing workflows, RFWI relies on the explicit scale separation between a smooth velocity macromodel and a rough reflectivity. This scale separation results from the gap between the wavenumber content of the velocity macromodel built by reflection tomography or migration velocity analysis and that of the reflectivity built by migration (Claerbout, 1985; Jannane et al., 1989). The scale separation leads to a two-step imaging workflow during which one repeatedly alternates the velocity model building assuming a known reflectivity and the reflectivity update by migration using the previous velocity update as the background model. One key limitation of RFWI, that will be overcome in this study, is the exclusive reliance on the use of reflected waves, discarding the low-wavenumber information on the shallow targets that are carried out by diving waves.
We propose to integrate ingredients of classical and reflection FWIs into a unified joint full waveform inversion (JFWI). As RFWI, JFWI still rests on a scale separation between the velocity macromodel and the reflectivity. The added-value of JFWI compared to RFWI is the combination of diving waves and reflected waves such that the long-wavelength information carried out by these two kinds of waves, as described above, are used for the velocity model building task in a way that is consistent with the coverage provided by the acquisition setup. A key feature of JFWI is the explicit separation of early arriving phases (diving waves and post-critical reflections) and pre-critical reflections in the data that allows us to filter out unwanted migration isochrones during the velocity model building step. We generate the reflectivity, which is required as a prior by JFWI, by classical FWI of reflected waves (i.e., least-squares migration) at each iteration of the scale-separation workflow. The two-step workflow has deep root in the theory of multi-parameter FWI through the use of the velocity-impedance parameterization which favors the scale separation between the smooth velocity model and the short-scale impedance model. The long-to-intermediate wavelengths of the velocity model that have been updated by JFWI can be further used as an initial model for classical FWI to build a broadband velocity model with a velocity-density parameterization.

Optimization formulation

FWI is a data-fitting procedure during which the subsurface model m is iteratively updated in order to match the synthetic data $d = d(m)$ with the recorded data d_{obs}. The misfit function is conventionally defined as the least-squares norm of the data residuals weighted by a linear operator W, that is

$$C_{FWI}(m) = \frac{1}{2} \left\| W \left(d_{obs} - d(m) \right) \right\|_2^2, \tag{1}$$

with implicit summation over sources, receivers and time. The sensitivity kernel of FWI is shown in Fig. 1a when the residual seismogram contains a diving-wave and a reflection components. It shows the wide first Fresnel zone, generated by the diving wave residual, whose illumination in depth is controlled by the source-receiver offset and the frequency, and a short-scale migration isochrone generated by the reflection residual.

Reflection FWI focuses on reflection data to build the subsurface model. The method relies on the prior knowledge of the reflectivity which is used as secondary sources in depth. The misfit function is given by

$$C_{RFWI}(m_0) = \frac{1}{2} \left\| W^r \left(d_{obs}^{refl} - d_{pred}^{refl}(m_0, \delta m) \right) \right\|_2^2, \tag{2}$$

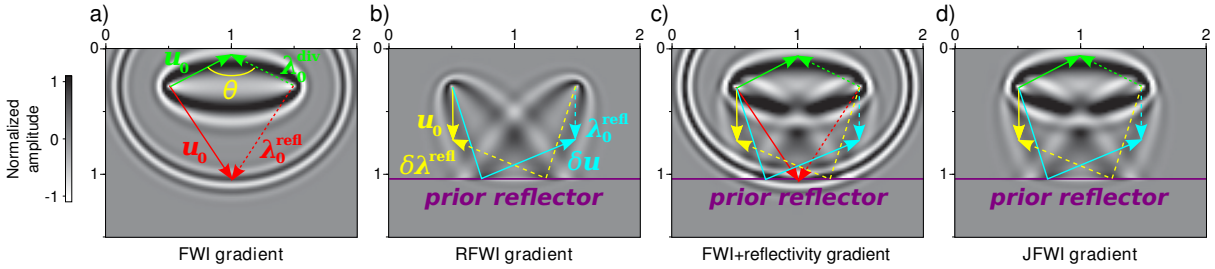

Figure 1 *Gradients generated by different FWI approaches. Solid and dashed arrows denote the ray paths respectively followed by the incident and adjoint fields that interfere constructively. (a) FWI gradient combines a low-wavenumber first Fresnel zone (represented by $u_0 \star \lambda_0^d$) between source and receiver, and a high-wavenumber migration isochrone (represented by $u_0 \star \delta\lambda^r$). The first Fresnel zone has a limited penetration in depth. (b) RFWI gradient shows two first Fresnel zones centered on the two-way path followed by the reflected wave between the reflector and the shot/receiver positions. (c) FWI gradient, with a prior reflectivity in the initial model, combines FWI and RFWI gradients. Low-wavenumber and high-wavenumber information enter into the gradient, hence breaking down the scale-separation prerequisite.(d) JFWI gradient combines the first Fresnel zone generated by direct-wave residuals and RFWI gradient. Compared with (c) the migration isochrone was removed to honor the scale separation.*

where d_{obs}^{refl} and d_{pred}^{refl} denote the observed and predicted reflected waves, respectively, weighted by the linear operator W^r. The low-wavenumber background m_0 and the high-wavenumber reflectivity δm are separated in scales, and RFWI seeks to reconstruct the background m_0 only using the two transmitted wavepaths connecting the reflectivity to the source and receiver (Fig. 1b).

The governing idea of Joint FWI is to explicitly separate the contribution of the diving waves and the reflected waves in the misfit function. This explicit data separation allows us to combine the sensitivity kernels of classical FWI and RFWI such that only the forward-scattered (transmission) wavepaths (the first Fresnel zone in Fig. 1a and the wavepaths of Fig. 1b) contribute to the JFWI sensitivity kernel at the expense of the back-scattered wavepaths (the migration isochrone in Fig. 1a). The filtering of the isochrone component performed by the data separation is highlighted by comparing the sensitivity kernels of the classical FWI and JFWI when a prior reflectivity is set in the background model (Figs. 1c and 1d).

The data separation leads to the following misfit function, which is decomposed as the sum of two terms,

$$C_{JFWI}(m_0) = \frac{1}{2}\left\| W^d \left(d_{obs}^{div} - d_{pred}^{div}(m_0) \right) \right\|_2^2 + \frac{1}{2}\left\| W^r \left(d_{obs}^{refl} - d_{pred}^{refl}(m_0, \delta m) \right) \right\|_2^2, \quad (3)$$

where d_{obs}^{div} and $d_{pred}^{div}(m_0)$ denote the observed and predicted diving waves, respectively. Respective contributions of the two terms in Equation (3) can be balanced by the weighting operators W^d and W^r. As we solve the forward problem in the time domain, this splitting operation can be performed by a simple linear time-offset windowing.

The gradient of the misfit function with respect to the background model m_0 is given by

$$\nabla C_{JFWI} = u_0 \star \lambda_0^d + u_0 \star \delta\lambda^r + \delta u \star \lambda_0^r + \delta u \star \delta\lambda^r, \quad (4)$$

where scalars λ_0^d and λ_0^r denote the background components of the adjoint field generated by the diving-wave residuals and the reflection residuals, and scalar $\delta\lambda^r$ denotes the scattered component of the adjoint wavefield generated by the reflection residuals, respectively. The first term in Equation (4) builds the first Fresnel zone associated with the diving waves, while the second and third terms are those generated during RFWI. The key point is that the gradient in Eq. (4) does not include the $u_0 \star \lambda_0^r$ term associated with the high-wavenumber migration isochrone (Fig. 1d).

Synthetic Valhall case study

We illustrate this workflow on a synthetic 2D Valhall model (Fig. 2(d,f)). Initial V_p model is a simple 1D model, chosen such that no cycle-skipping occurs on direct and diving waves. The maximum offset in the acquisition is 6km such that diving waves only sample the upper part of the subsurface. The first high-wavenumber I_P model is built by classical FWI of the short-offset reflected waves, namely by least-squares migration. The misfit function (i.e. eq. (1)) decreased by 50% in only 5 iterations as the I_P inversion is a quite linear problem. This first impedance

model is then used as fixed prior perturbation model to compute the gradient of the JFWI misfit function from which the long wavelengths of V_P are updated from both the diving waves and reflected waves. We iteratively cycle the high-wavenumber I_p reconstruction and the low-wavenumber V_p reconstruction until convergence of the two optimizations. The two final V_p and I_p JFWI images are shown in Figure 2(c,e). We also display the FWI and RFWI V_p velocity models in Figs. 2(a-b) for comparison with the JFWI results. We first show that classical FWI remains stuck in a local minimum due to the poor accuracy of the initial model and the lack of low frequencies (Figs 2a). Second, we show how accounting for the diving waves in JFWI improves the shallow reconstruction of V_P compared to RFWI (compare Figs. 2b and 2c). These shallow improvements turn out to have significant impact on the accuracy of the impedance image deeper (Fig. 2e).

Conclusions and perspectives

We propose to build the velocity macromodel by a specific formulation of full waveform inversion by joint inversion of diving waves and reflected waves. Our approach relies on the explicit scale decomposition of the subsurface model into a smooth background velocity model and reflectivity, and a hierarchical subdivision of seismic dataset into diving waves and short-spread reflected waves. These decompositions make the velocity gradient to be dominated by surface-to-surface and reflector-to-surface first Fresnel zones. We propose a computationally efficient implementation of this approach which requires twice the cost of the classical FWI, aside the like-migration procedure for the I_p reconstruction, leading us to think that 3D extension is manageable. This unified formulation for the velocity analysis is integrated into a hierarchical workflow that alternates impedance and velocity updates. We illustrate on a synthetic case that the specific subsurface parameterization drives the FWI toward the reconstruction of the long wavelengths.

Acknowledgments

This study was funded by the SEISCOPE consortium (*http://seiscope2.osug.fr*), sponsored by BP, CGG, CHEVRON, EXXON-MOBIL, JGI, PETROBRAS, SAUDI ARAMCO, SCHLUMBERGER, SHELL, SINOPEC, STATOIL, TOTAL and WOODSIDE. This study was granted access to the HPC resources of CIMENT infrastructure (https://ciment.ujf-grenoble.fr) and CINES/IDRIS under the allocation 046091 made by GENCI.

References

Almomin, A. and Biondi, B. [2012] Tomographic Full Waveform Inversion: Practical and Computationally Feasible Approach. *SEG Technical Program Expanded Abstracts*, 1–5.

Biondi, B. and Almomin, A. [2012] Tomographic full waveform inversion (TFWI) by combining full waveform inversion with wave-equation migration velocity analysis. *SEG Technical Program Expanded Abstracts*, 1–5.

Brossier, R., Operto, S. and Virieux, J. [2014] Velocity model building from seismic reflection data by full waveform inversion. *Geophysical Prospecting*, doi = 10.1111/1365-2478.12190,.

Chavent, G., Clément, F. and Gòmez, S. [1994] Automatic determination of velocities via migration-based traveltime waveform inversion: A synthetic data example. *SEG Technical Program Expanded Abstracts*, 1179–1182.

Claerbout, J. [1985] *Imaging the Earth's interior*. Blackwell Scientific Publication.

Jannane, M., Beydoun, W., Crase, E., Cao, D., Koren, Z., Landa, E., Mendes, M., Pica, A., Noble, M., Roeth, G., Singh, S., Snieder, R., Tarantola, A. and Trezeguet, D. [1989] Wavelengths of Earth structures that can be resolved from seismic reflection data. *Geophysics*, **54**(7), 906–910.

Ma, Y. and Hale, D. [2013] Wave-equation reflection traveltime inversion with dynamic warping and full waveform inversion. *Geophysics*, **78**(6), R223–R233.

Sava, P. and Biondi, B. [2004] Wave-equation migration velocity analysis. I. Theory. *Geophysical Prospecting*, **52**(6), 593–606.

Sava, P. and Fomel, S. [2006] Time-shift imaging condition in seismic migration. *Geophysics*, **71**(6), S209–S217.

Sun, D. and Symes, W.W. [2012] Waveform Inversion via Nonlinear Differential Semblance Optimization. *SEG Technical Program Expanded Abstracts*, 1–7.

Symes, W.W. and Carazzone, J.J. [1991] Velocity inversion by differential semblance optimization. *Geophysics*, **56**, 654–663.

Virieux, J. and Operto, S. [2009] An overview of full waveform inversion in exploration geophysics. *Geophysics*, **74**(6), WCC1–WCC26.

Xu, S., Wang, D., Chen, F., Lambaré, G. and Zhang, Y. [2012] Inversion on Reflected Seismic Wave. *SEG Technical Program Expanded Abstracts*, 1–7.

Yang, T. and Sava, P. [2011] Wave-equation migration velocity analysis with time-shift imaging. *Geophysical Prospecting*, **59**(4), 635–650.

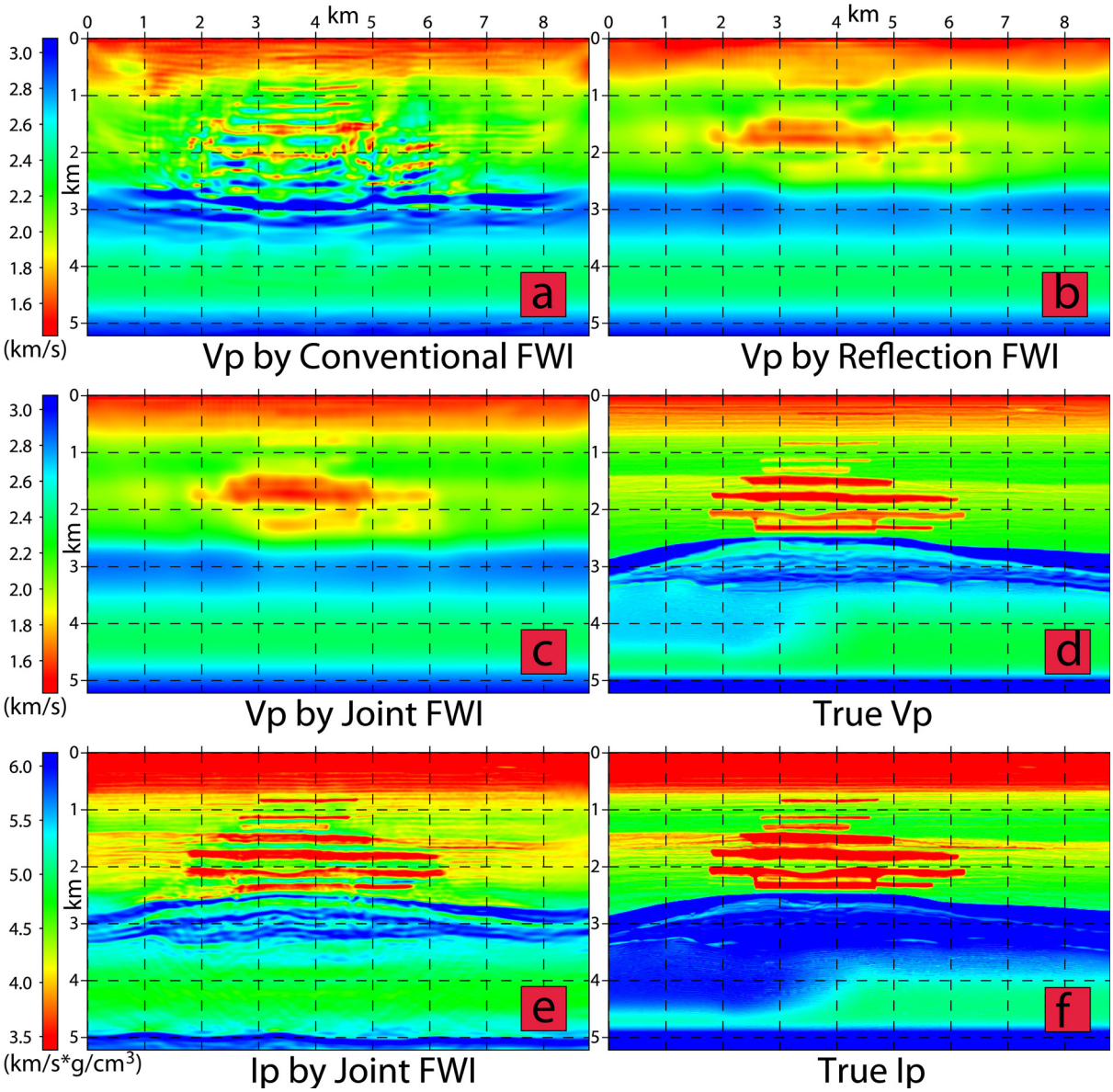

Figure 2 *(a) V_p built by classical FWI. (b) V_p built by RFWI. (c) V_p built by JFWI. Compared to (b), note the improvements in the shallow part. (d) True V_P. (e) Final I_P model built by classical FWI of short-offset reflected waves using the JFWI V_P model (c) as background model. (f) Trup I_P.*